Bayesian Calibration and Bias Correction for Forward Model-driven SHM

PAUL GARDNER, ROBERT J. BARTHORPE
and CHARLES LORD

ABSTRACT

Forward model-driven structural health monitoring (SHM) is an alternative approach to the two main categories of SHM research: model-driven and data-driven processes. It is a methodology whereby a validated numerical model is used, in a forward manner, in order to produce simulated damage state data for machine learning applications. This paper explores the use of Bayesian calibration and bias correction (BCBC) in order to simulate representative predictions of observational data. The technique allows calibration of a numerical model to be performed in a Bayesian scheme whilst accounting for bias that may occur due to simplifications of the underlying physics in the model. This paper demonstrates the application of BCBC, in a forward model-driven framework, for producing representative damage features for different damage extents and shows a comparison with both experimental and non-bias corrected damage features.

INTRODUCTION

Two main categories of approaches to structural health monitoring (SHM) exist: data-driven and model-driven processes. Data-driven methodologies use pattern recognition or machine learning techniques in order to make decisions from observational data [1]. Conversely, model-driven frameworks seek to update parameters associated with law-based models using an inverse methodology; these updated parameters are used to infer damage [2]. Both frameworks suffer from disadvantages. Data-driven methods require data from all potential damage scenarios; this is often costly and infeasible. Model-driven approaches, in contrast, are challenged with issues of parameter non-identifiability and interpretability as well as handling experimental variabilities. Forward model-driven SHM seeks to address these issues by using numerical models, in a forward manner, in order to produce predictive damage features that are representative of those obtained experimentally. These predictive damage features are then used

Paul Gardner, Dynamics Research Group, University of Sheffield, Mappin Street, Sheffield, S1 3JD, U.K..
Email: pagardner1@sheffield.ac.uk
Robert J. Barthorpe, Dynamics Research Group, University of Sheffield.
Charles Lord, Dynamics Research Group, University of Sheffield.

as training data in machine learning applications. To generate damage features that are statistically similar to those obtained experimentally, the focus of this paper, Bayesian calibration and bias correction (BCBC) is implemented in the forward model-driven framework. BCBC calibrates numerical models whilst accounting for simplifications in the underlying physics. This paper demonstrates that BCBC generates more representative damage features compared to non-bias corrected Bayesian calibration (BC).

BAYESIAN CALIBRATION AND BIAS CORRECTION

BCBC defines the relationship between experimental (or observational) data $\mathbf{z}$, and numerical model outputs $\eta(\mathbf{x}, \boldsymbol{\theta})$, as shown in Equation 1 [3–5].

$$z(\mathbf{x}) = \zeta(\mathbf{x}) + e = \rho\eta(\mathbf{x}, \boldsymbol{\theta}) + \delta(\mathbf{x}) + e \tag{1}$$

Equation 1 states that experimental data at some set of inputs $\mathbf{x}$, is equal to the 'true' underlying process $\zeta(\mathbf{x})$, with the addition of experimental variability e (assumed to be independently distributed Gaussian distributions, $\mathcal{N}(0, \lambda)$). This 'true' process is equal to a calibrated numerical model $\eta(\mathbf{x}, \boldsymbol{\theta})$ (where $\boldsymbol{\theta}$ is a set of calibrated parameters) with the inclusion of a bias (or model discrepancy) term $\delta(\mathbf{x})$. The regression parameter ρ weights the importance of the model discrepancy term.

Complex numerical models, where for a set of inputs the output is not known until it is run, e.g. finite element (FE) models, are referred to as simulators. To reduce the computational expense of running a simulator an emulator is used. An emulator is a regression model that can be fit to simulator runs $\eta(\mathbf{x}_*, \mathbf{t})$ and interpolate efficiently across the parameter space. Here $\mathbf{x}_*$ are simulator run inputs, $\mathbf{t}$ are potential calibration parameters and $\mathbf{x}$ are inputs where experimental data has been collected. In BCBC the emulator is a Gaussian Process (GP) regression model, adopted due their flexibility and non-parametric form. Prior information about the simulator and model discrepancy are modelled as GPs as shown in Equations 2 and 3.

$$\eta(\mathbf{x}_*, \mathbf{t}) \sim GP(m_1(\mathbf{x}_*, \mathbf{t}), c_1[(\mathbf{x}_*, \mathbf{t}), (\mathbf{x}'_*, \mathbf{t}')]) \tag{2}$$

$$\delta(\mathbf{x}) \sim GP(m_2(\mathbf{x}), c_2(\mathbf{x}, \mathbf{x}')) \tag{3}$$

The mean functions, $m_1(\cdot)$ and $m_2(\cdot)$, and covariances functions, $c_1(\cdot, \cdot)$ and $c_2(\cdot, \cdot)$ used, are constant mean and Gaussian covariance functions as shown in Equations 4 and 5. A constant mean function is used due to limited *a priori* knowledge of the simulator and discrepancy functional forms. Gaussian covariance functions represent the prior belief that the simulator and discrepancy will have relatively smooth functional forms.

$$m(\mathbf{x}) = \mathbf{H}\boldsymbol{\beta} \tag{4}$$

$$c(\mathbf{x}, \mathbf{x}') = \sigma^2 \exp[-(\mathbf{x} - \mathbf{x}')^T \Omega (\mathbf{x} - \mathbf{x}')] \tag{5}$$

Where $\mathbf{H}$ is a design matrix and $\boldsymbol{\beta}$ are scaling coefficients; for a constant mean function $H(x) = 1$. The hyperparameters σ^2 and Ω are the scale factor and a diagonal matrix of roughness parameters[1] respectively. In order to preserve conciseness of this paper, the reader is referred to [6, 7] for more information on GPs.

The BCBC methodology can be separated into four main stages as outlined:

[1]Where $\Omega_{ii} = \omega_i$ for $i = 1, \ldots, D$ and D is the dimensionality of input $\mathbf{x}$.

Stage 1: The simulator is run over a finite set of plausible inputs $\mathbf{x}_*$, and calibration parameters $\mathbf{t}$, in order to obtain a set of outputs $\mathbf{y}$. A GP emulator is fitted to the simulator runs via optimising the hyperparameters $\boldsymbol{\phi}_1 = [\boldsymbol{\beta}_1, \sigma_1^2, \Omega_{x_*}, \Omega_t]$ to maximise the marginal likelihood.

Stage 2: The experimental data $\mathbf{z}$, obtained for inputs $\mathbf{x}$, is statistically modelled with three components as to satisfy Equation 1; the prior of this model is shown in Equation 6. The first component is the GP emulator from stage 1 with fixed hyperparameters $\boldsymbol{\phi}_1$. The second and third components are a GP that represents the model discrepancy $\delta(\mathbf{x})$ with a variance term λ modelling the experimental variability; governed by the hyperparameters $\boldsymbol{\phi}_2 = [\boldsymbol{\beta}_2, \sigma_2^2, \Omega_x, \lambda, \rho]$. In order to make inference about model discrepancy the calibration parameters $\mathbf{t}$ are marginalised out of the GP emulator component with respect to the prior of $\boldsymbol{\theta}$. The hyperparameters $\boldsymbol{\phi}_2$, are subsequently optimised in order to maximise the marginal likelihood of the statistical model.

$$\mathbf{z} \sim GP\left((\rho m_1(\mathbf{x}_*, \mathbf{t}) + m_2(\mathbf{x}, \mathbf{t})), (\rho c_1[(\mathbf{x}_*, \mathbf{t}), (\mathbf{x}'_*, \mathbf{t}')] + c_2(\mathbf{x}, \mathbf{x}') + \mathbf{I}\lambda)\right) \quad (6)$$

Stage 3: Inference about the calibration parameters $\boldsymbol{\theta}$ is performed as in Equation 7, with fixed optimised hyperparameters $\hat{\boldsymbol{\phi}} = [\hat{\boldsymbol{\phi}}_1, \hat{\boldsymbol{\phi}}_2]$. This results in an empirical Bayes approach as marginalising out the hyperparameters $\boldsymbol{\phi}$ would result in a highly intractable function. The simulator and experimental outputs are combined so that $\mathbf{d} = [\mathbf{y}^T, \mathbf{z}^T]^T$. Equation 7 is evaluated using a Gauss-quadrature method due to its intractability. Here a maximum *a posteriori* (*MAP*) estimate is used for the calibrated parameters.

$$p(\mathbf{d}|\hat{\boldsymbol{\phi}}) = \int p(\mathbf{d}|\boldsymbol{\theta}, \hat{\boldsymbol{\phi}}) p(\boldsymbol{\theta}) d\boldsymbol{\theta} \quad (7)$$

Stage 4: Inference about the calibrated prediction of the experimental data is performed. The unconditional predictive posterior distribution is formed by marginalising the conditional posterior, with respect to the posterior distribution of the calibration parameters, $p(\boldsymbol{\theta}|\hat{\boldsymbol{\phi}}, \mathbf{d})$. This is an intractable function and so a Gauss-quadrature method is used to perform inference.

Due to limitations of the scope of this paper, the reader is referred to [3, 8] for full mathematical descriptions of the BCBC approach.

Numerical Example

Forward model-driven SHM requires that a simulator produces representative predictions of damage features. Here BCBC is demonstrated for a mass and tensioned wire system illustrating the methods ability to replicate experimental data. Figure 1 shows two scenarios of a mass, tensioned wire system; with a centred and off-centred mass, Figures 1a and 1b respectively. The two scenarios correspond to a simulator (Figure 1a)

(a) (b)

Figure 1: Mass, tensioned wire system: (a) simulator; centred mass, tensioned wire, (b) 'true' process; off-centred mass, tensioned wire. (L=1m a=0.2m).

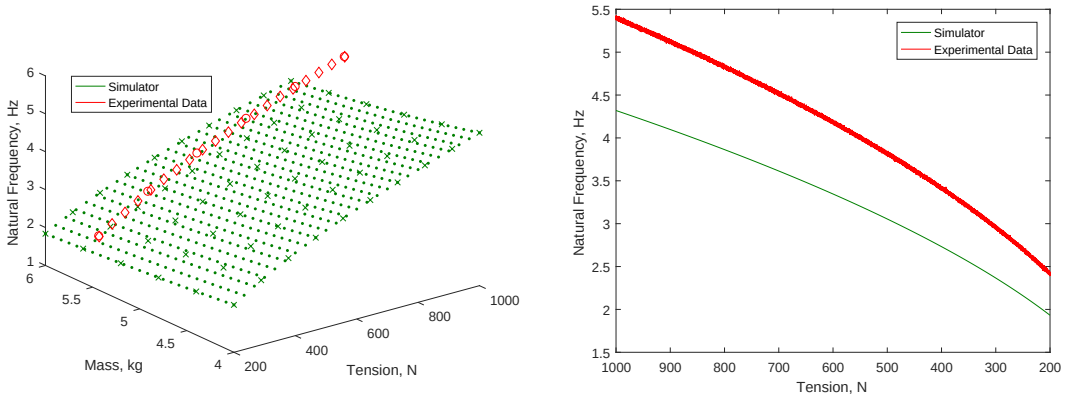

(a) (b)

Figure 2: Mass, tension wire system: (a) simulator training ($\times$), testing ($\cdot$) and experimental training ($\circ$), testing ($\diamond$) points, (b) comparison of simulator $\eta(\mathbf{x}_*, 5.43)$ and experimental data.

and 'true' process (Figure 1b). The simulator contains a simplification of the physics of the 'true' process, an assumption that the mass will be centred, creating the model discrepancy shown in Figures 2. The tension in the wires T are the inputs $\mathbf{x}_*$ and $\mathbf{x}$ (a reduction representing damage), and the mass of the system m is the calibration parameter $\mathbf{t}$; the 'true' mass being 5.43kg. The damage feature is the natural frequency of the system ω; calculated for each scenario as shown in Equations 8 and 9 respectively. Experimental data $\mathbf{z}$ are simulated from the 'true' process (Equation 9) with the inclusion of Gaussian distributed noise, $\mathcal{N}(0, 0.0001)$. To obtain training data the simulator (Equation 8) was run for a combination of ten equally spaced inputs between 1000-200N and six equally spaced calibration parameters between 4-6kg. The experimental training data was six equally spaced tensions between 1000-200N. The training and testing data is displayed in Figure 2a. The prior for the mass was $m \sim \mathcal{N}(5.93, 10)$.

$$\omega_c = \frac{1}{\pi}\left(\frac{T}{mL}\right)^{\frac{1}{2}} \tag{8}$$

$$\omega_{oc} = \frac{1}{2\pi}\left(\frac{T(a+b)}{mab}\right)^{\frac{1}{2}} \tag{9}$$

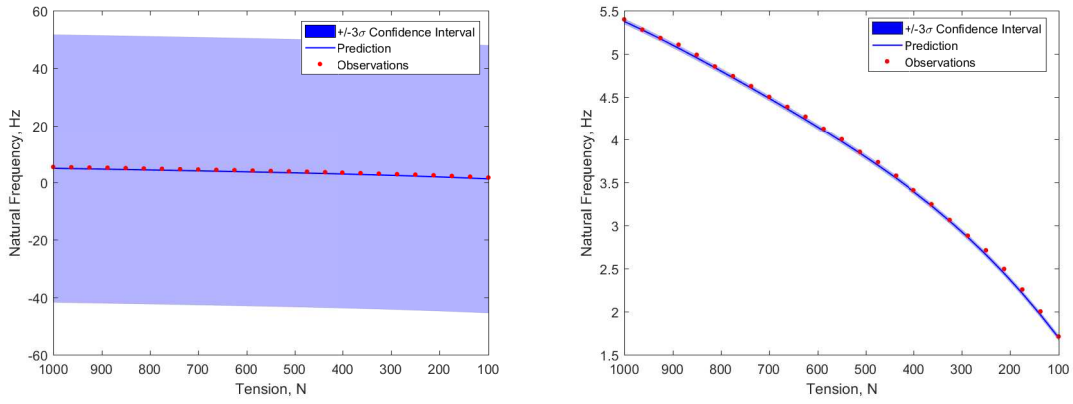

(a) (b)

Figure 3: BCBC predictions: (a) with numerical issues, (b) with current solution.

In Figure 3a issues in the prediction on test data occur due to numerical instabilities in inverting poorly conditioned covariance matrices in the emulator, an area of further research. To demonstrate the application of the method a current solution is to include a constant, the residual between the mean of the prediction and the mean of the training experimental data, which has been shown to generalise well. Figure 3b shows the BCBC prediction with the inclusion of this constant, the normalised mean squared error (NMSE) is 0.07 and the calibrated mass is 5.89kg. The confidence intervals in Figure 3b are estimated from the variance of the experimental training data. It is noted that issues of non-identifiability between the calibration parameter and model discrepancy exist.

Importance of Incorporating Model Discrepancy

The importance of the model discrepancy term is demonstrated for the numerical example using BC for two scenarios. The first scenario, where the simulator and 'true' process are both defined by Equation 9. The second scenario, where the simulator and 'true' process are defined by Equation 8 and 9 respectively. The simulator and experimental inputs, the experimental noise and prior $p(\boldsymbol{\theta})$, are the same as in the previous example. BC is performed by obtaining the *MAP* estimate of $\boldsymbol{\theta}$ via optimisation as shown in Equation 10 [9] where the likelihood is as shown in Equation 11. The function $f(\boldsymbol{\theta})$ is a GP emulator and n is the number of experimental observations.

$$[\boldsymbol{\theta}_{MAP}, \lambda_{MAP}] = \arg\max_{\boldsymbol{\theta},\lambda} p(\boldsymbol{\theta}|\mathbf{z}) = \arg\max_{\boldsymbol{\theta},\lambda} p(\mathbf{z}|\boldsymbol{\theta})p(\boldsymbol{\theta}) \tag{10}$$

$$p(\mathbf{z}|\boldsymbol{\theta}) = \frac{1}{(2\pi\lambda^2)^{n/2}} \exp\left[\frac{-\sum_{i=1}^{n}\left(z_i - f_i(\boldsymbol{\theta})\right)^2}{2\lambda^2}\right] \tag{11}$$

Figures 4a and 4b show the calibrated predictions for the two scenarios. Figure 4a demonstrates that when the simulator has the same functional form as the experimental data calibration is possible, exhibited by a calibrated mass of 5.43kg and NMSE of 0.02. Figure 4b shows that worse predictions will be made when model discrepancy exists, demonstrated by a calibrated mass of 4.89kg and NMSE of 2.47. This states that the incorporation model discrepancy is important if accurate predictions of observational

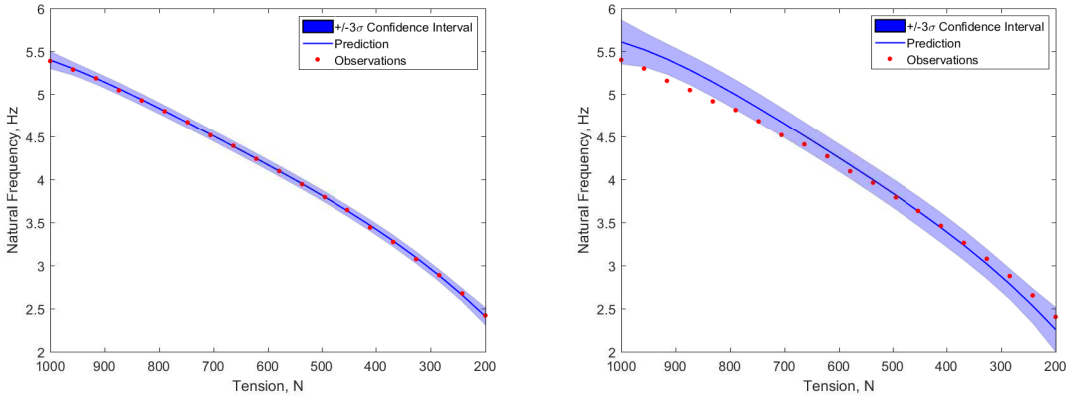

(a) (b)

Figure 4: BC predictions: (a) both simulator and 'true' process have the same functional form, (b) model discrepancy between simulator and 'true' process.

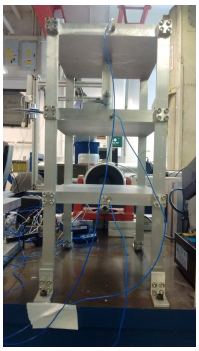

Figure 5: Experimental setup for the representative three storey building structure.

TABLE I: TRAINING DATA FOR BCBC AND BC.

SIMULATOR

Inputs $\mathbf{x}_*$	Calibration Parameters $\mathbf{t}$	Output $\mathbf{y}$
Damage Depths, $0, 2.5, \cdots, 20$mm	E, $65, 66, \cdots, 71$GPa	ω_3, Hz

EXPERIMENTAL

Inputs $\mathbf{x}$	Output $\mathbf{z}$
Damage Depths $0, 5, 20$mm	$\bar{\omega}_3$, Hz

data are required, as is the case in forward model-driven SHM. For further examples on the importance of model discrepancy see [10].

DAMAGE FEATURE PREDICTIONS FOR DIFFERENT DAMAGE EXTENTS

BCBC is used in order to produce predictive damage features from a simulator that are representative of those obtained experimentally, a key part of forward model-driven SHM. Modal testing of a representative building structure made from aluminium 6082, shown in Figure 5, was performed for nine damage extents and the first three bending natural frequencies obtained. The damage extents were saw cuts of 2.5mm from 0-20mm in the front right beam of Figure 5. The structure was excited using broadband noise via an electrodynamic shaker and the response measured by three accelerometers at each of the floors. Five measurement repeats were made for each damage extent. For visualisation reasons, the damage feature is simplified to the third natural frequency ω_3, due to it having the largest reduction when damage was introduced.

The simulator was a modal FE model where each damage state was modelled geometrically, i.e. the geometry of the saw cut was included in that of the beam. The training data for both BC and BCBC are shown in Table I; requiring 63 FE model runs and three experimental data points (the averaged natural frequency at three damage states, $\bar{\omega}_3$). The validation data was five repeats for all nine experimental damage extents. The prior

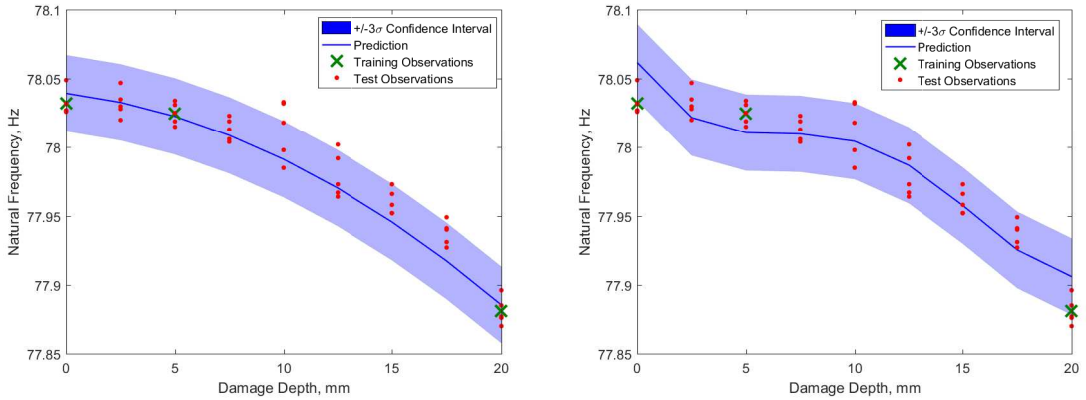

(a) (b)

Figure 6: Natural frequency against damage depth: (a) BCBC prediction, (b) BC prediction.

for the elastic modulus was $E \sim \mathcal{N}(66, 1)$. The variance for both methods was estimated from the three training damage extents, due to the numerical issues in the BCBC method; for this reason interest is largely restricted to mean predictions. The predictions for BCBC and BC are shown in Figures 6a and 6b. The NMSE was calculated between the prediction and the five experimental repeats for each approach. The average NMSE for the BCBC and BC methods were 9.47 and 14.30; the calibrated elastic moduli were 65.95GPa and 69.42GPa respectively.

Comparison of Predicted Feature Distributions for Each Damage Extent

To assess both the training and validation points of the BCBC and BC predictions, the posterior distributions for each damage extent were compared with both kernel density estimates (KDEs) (using a normal kernel function) and Gaussian approximations of the experimental data; visualised in Figure 7. Table II presents the means of the Gaussian approximation and posterior distributions from the BCBC and BC predictions along with the Kullback-Leibler (KL) divergence ($\mathbb{KL}$) when each is compared to the KDEs as well as the absolute average percentage difference $\bar{\%}$ and summed KL divergence $\sum \mathbb{KL}$. The KL divergence shown in Equation 12 is a measure of relative entropy [11] (where K is the number of states for a discrete variable) and a comparison is displayed in Figure 8. It is the average number of extra bits (binary digits) required to encode the data given that distribution q is used to model the 'true' distribution p. If the KL divergence is equal to zero then $q = p$.

$$\mathbb{KL}\left(p||q\right) = \sum_{k=1}^{K} p_k \log\left(\frac{p_k}{q_k}\right) \tag{12}$$

DISCUSSION AND CONCLUSIONS

Damage feature prediction was performed for a three storey representative building structure using both BCBC and BC approaches as part of the first stages of forward model-driven SHM. The visual comparison in Figure 7, the KL-divergences when compared to the KDEs in Figure 8 and Table II, demonstrate that apart from the 0mm damage

TABLE II: COMPARISON OF DISTRIBUTIONS. * DENOTES TRAINING DATA DEPTHS.

	Experimental Data		BCBC			BC		
Damage Depth, mm	Mean, Hz	$\mathbb{KL}$, bits	Mean, Hz	%	$\mathbb{KL}$, bits	Mean, Hz	%	$\mathbb{KL}$, bits
0.0*	78.032	1.548	78.039	0.009%	1.980	78.062	0.038%	8.949
2.5	78.032	0.037	78.033	0.001%	0.067	78.022	-0.013%	0.942
5.0*	78.025	0.085	78.023	-0.003%	0.056	78.011	-0.018%	1.681
7.5	78.013	0.141	78.009	-0.005%	0.195	78.010	-0.004%	0.127
10.0	78.013	0.072	77.991	-0.028%	7.364	78.005	-0.011%	3.955
12.5	77.980	0.068	77.970	-0.012%	1.859	77.987	0.009%	1.569
15.0	77.960	0.059	77.946	-0.019%	1.876	77.958	-0.003%	0.116
17.5	77.938	0.287	77.917	-0.026%	3.710	77.925	-0.016%	1.481
20.0*	77.881	0.069	77.885	0.006%	0.314	77.906	0.032%	5.490
$\sum \mathbb{KL}$		2.366			17.422			24.310
$\bar{\%}$				0.012%			0.016%	

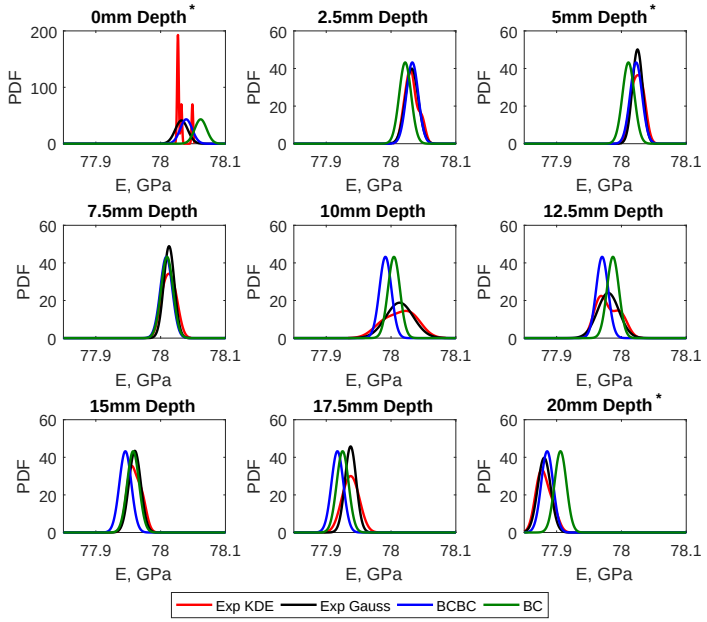

Figure 7: Comparison of distributions for each damage depth; Exp KDE - KDE for experimental data, Exp Gauss - Gaussian approximation of experimental data. * denotes training data depths.

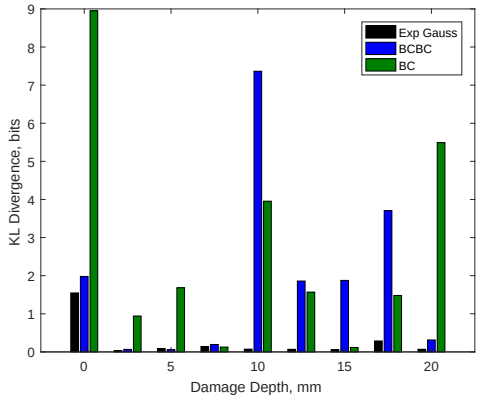

Figure 8: Comparison of KL divergence from KDE for each damage depth; Exp Gauss - Gaussian approximation of experimental data.

extent a Gaussian approximation is reasonable for the experimental data. This confirms that a posterior Gaussian assumption is appropriate for this damage feature. A KDE should be fit with more than five data points and therefore given more data, the first damage state distribution may tend towards a Gaussian distribution.

BCBC produced more representative damage features when compared with BC, displaying the importance of model discrepancy; demonstrated by lower absolute average percentage differences in Table II and lower average NMSE. The KL divergences in Figure 8 and a visual comparison in Figure 7 indicate that BCBC also more accurately replicated the experimental distributions; highlighted by a lower summed KL divergence. The comparable KL divergences in Figure 8 and Table II between BCBC and the experimental Gaussian approximation for the first four and last damage extents evidences that BCBC produces damage features representative of those obtained experimentally. However, a wide discrepancy is seen for the 10-17.5mm damage extents. This is likely to be

due to the lack of experimental data used to fit the 'true' distribution. Another cause may be due to differences in the variance, due to the assumption of a fixed variance caused by the numerical issues in BCBC. The numerical example provided further evidence of the importance of the bias term. Conventional calibration, when the functional form of the simulator and 'true' underlying process are different, will lead to overfitting. Accordingly, BCBC is a more suitable modelling approach for producing representative damage state features in a forward model-driven SHM framework.

Several areas of further research have been highlighted. Firstly, the process currently requires experimental training data - albeit a much smaller set than a data-driven approach. Consequently, an area of further research is in scaling BCBC subsystem models to full system model predictions whilst accounting for model discrepancy between subsystem layers in a similar framework to Strong et al. [12]. This approach would mean that only component level damage state data would be required for full system predictions. Secondly, identifiability issues have been observed between the model discrepancy and calibrated parameters. This may be improved by incorporating multiple output GPs [13, 14], and therefore more clearly defining the model discrepancy and reducing the amount of plausible calibration parameters. Finally, methods for dealing with the numerical instabilities from the application of BCBC (from the inverting of poorly-conditioned covariance matrices) is an area for further research.

REFERENCES

1. Worden, K. and G. Manson. 2007. "The application of machine learning to structural health monitoring," *Philosophical Transactions of the Royal Society of London A: Mathematical, Physical and Engineering Sciences*, 365(1851):515–537.
2. Friswell, M. I. 2007. "Damage identification using inverse methods," *Philosophical Transactions of the Royal Society of London A: Mathematical, Physical and Engineering Sciences*, 365(1851):393–410.
3. Kennedy, M. C. and A. O'Hagan. 2001. "Bayesian calibration of computer models," *Journal of the Royal Statistical Society: Series B (Statistical Methodology)*, 63(3):425–464.
4. Bayarri, M. J., J. O. Berger, R. Paulo, J. Sacks, J. A. Cafeo, J. Cavendish, C.-H. Lin, and J. Tu. 2007. "A Framework for Validation of Computer Models," *Technometrics*, 49(2):138–154.
5. Arendt, P. D., D. W. Apley, and W. Chen. 2012. "Quantification of Model Uncertainty: Calibration, Model Discrepancy, and Identifiability," *Journal of Mechanical Design*, 134:100908–100908–12.
6. Rasmussen, C. E. and C. K. I. Williams. 2006. *Gaussian Processes for Machine Learning*, The MIT Press.
7. Oakley, J. 2002. "Eliciting Gaussian process priors for complex computer codes," *Journal of the Royal Statistical Society Series D: The Statistician*, 51.
8. Kennedy, M. C. and A. O'Hagan. 2001. "Supplementary details on Bayesian Calibration of Computer Models," Tech. rep.
9. Smith, R. C. 2014. *Uncertainty Quantification: Theory, Implementation, and Applications*, SIAM.
10. Brynjarsdóttir, J. and A. O'Hagan. 2014. "Learning about physical parameters: The importance of model discrepancy," *Inverse Problems*, 30.
11. Murphy, K. P. 2012. *Machine Learning: A Probabilistic Perspective*, The MIT Press.
12. Strong, M., J. E. Oakley, and J. Chilcott. 2012. "Managing structural uncertainty in health economic decision models: a discrepancy approach," *Journal of the Royal Statistical Society: Series C (Applied Statistics)*, 61(1):25–45.
13. Arendt, P. D., D. W. Apley, W. Chen, D. Lamb, and D. Gorsich. 2012. "Improving identifiability in model calibration using multiple responses," *Journal of Mechanical Design*, 134:100909–100909–9.
14. Fricker, T. E., J. E. Oakley, and N. M. Urban. 2013. "Multivariate Gaussian Process Emulators With Nonseparable Covariance Structures," *Technometrics*, 55(1):47–56.